Victor Hugo Souza*, Taian Martins Vieira[a], André Salles Cunha Peres[a], Marco Antonio Cavalcanti Garcia, Claudia Domingues Vargas and Oswaldo Baffa

Effect of TMS coil orientation on the spatial distribution of motor evoked potentials in an intrinsic hand muscle

https://doi.org/10.1515/bmt-2016-0240
Received August 24, 2016; accepted July 3, 2017

Abstract: Previous reports on the relationship between coil orientation and amplitude of motor evoked potential (MEP) in transcranial magnetic stimulation (TMS) did not consider the effect of electrode arrangement. Here we explore this open issue by investigating whether TMS coil orientation affects the amplitude distribution of MEPs recorded from the abductor pollicis brevis (APB) muscle with a bi-dimensional grid of 61 electrodes. Moreover, we test whether conventional mono- and bipolar montages provide representative MEPs compared to those from the grid of electrodes. Our results show that MEPs with the greatest amplitudes were elicited for 45° and 90° coil orientations, i.e. perpendicular to the central sulcus, for all electrode montages. Stimulation with the coil oriented at 135° and 315°, i.e. parallel to the central sulcus, elicited the smallest MEP amplitudes. Additionally, changes in coil orientation did not affect the spatial distribution of MEPs over the muscle extent. It has been shown that conventional electrodes with detection volume encompassing the APB belly may detect representative MEPs for optimal coil orientations. In turn, non-optimal orientations were identified only with the grid of electrodes. High-density electromyography may therefore provide new insights into the effect of coil orientation on MEPs from the APB muscle.

Keywords: brain stimulation; conventional electrodes; electric field direction; high-density electromyography; muscle imaging; transcranial magnetic stimulation.

[a]**Taian Martins Vieira and André Salles Cunha Peres:** These authors contributed equally to this work
***Corresponding author: Victor Hugo Souza,** Departamento de Física, Faculdade de Filosofia, Ciências e Letras de Ribeirão Preto (FFCLRP), Universidade de São Paulo (USP), Av. Bandeirantes, 3900, 14040-901 Ribeirão Preto-SP, Brazil, Phone: +55 16 33153778, Fax: +55 16 33154887, E-mail: victorhos@hotmail.com. http://orcid.org/0000-0002-0254-4322
Taian Martins Vieira: Departamento de Arte Corporal, Escola de Educação Física e Desportos, Universidade Federal do Rio de Janeiro, Av. Carlos Chagas Filho, 540, 21941-599 Rio de Janeiro, RJ, Brazil; and Laboratorio di Ingegneria del Sistema Neuromuscolare, Dipartimento di Elettronica e Telecomunicazioni, Politecnico di Torino, Via Cavalli 22/H, 10138 Turin, Italy
André Salles Cunha Peres: Instituto Internacional de Neurociência de Natal Edmond e Lily Safra, Instituto Santos Dumont, Rodovia RN 160 Km 03, 3003, 59280-000 Macaíba-RN, Brazil
Marco Antonio Cavalcanti Garcia: Departamento de Biociências e Atividades Físicas, Escola de Educação Física e Desportos, Universidade Federal do Rio de Janeiro, Av. Carlos Chagas Filho, 540, 21941-599 Rio de Janeiro-RJ, Brazil. http://orcid.org/0000-0002-8225-6573
Claudia Domingues Vargas: Instituto de Biofísica Carlos Chagas Filho, Universidade Federal do Rio de Janeiro, Av. Carlos Chagas Filho, 373, 21941-902 Rio de Janeiro-RJ, Brazil
Oswaldo Baffa: Departamento de Física, Faculdade de Filosofia, Ciências e Letras de Ribeirão Preto, Universidade de São Paulo, Av. Bandeirantes, 3900, 14040-901 Ribeirão Preto, SP, Brazil

Introduction

Transcranial magnetic stimulation (TMS) is a powerful tool for non-invasive and painless brain stimulation [3, 14, 52]. Magnetic pulses generated by a coil positioned non-invasively over the primary motor cortex induce electric fields in the cortical tissue, depolarizing neurons. The resulting action potentials descend along the corticospinal tract reaching the spinal motor neurons and, ultimately, the target muscles. The myoelectric activity produced in response to TMS pulses is named motor evoked potential (MEP) and is commonly recorded by surface electrodes [14, 39, 53]. Peak-to-peak amplitude and latency extracted from MEPs of intrinsic hand muscles are of major clinical interest and have been used to study brain physiology [40] and to assess damage to the motor cortex and corticospinal tract [39, 55].

However, MEP properties are highly sensitive to stimulation parameters [5, 34], in particular, to the coil orientation. For instance, there is a consensus that the optimal coil orientation to elicit MEPs with maximum amplitude in thenar hand muscles is around 45° away from the sagittal plane [2, 4, 30]. Such reasoning is based on the direction

of the current produced when the electric field is induced perpendicularly to the central sulcus wall. In this case, current lines are oriented parallel to a greater number of neuronal axons, leading to MEPs with higher amplitude in the target hand muscles [2, 4, 8, 22, 33]. MEPs also exhibit different latencies according to pulse direction [7, 11, 54], suggesting that different TMS orientations may activate different cortical neural elements and distinct populations of motor neurons [7, 11]. It is possible, then, that for each coil orientation, motor neurons supplying distinct motor units with different properties are activated.

Previous studies evaluated the effect of coil orientation on MEP amplitude using one (monopolar) or two (bipolar montage) surface electrodes. Signals of conventional electrodes are an average of myoelectric potentials from active muscle fibers within a particular detection volume under the skin surface [45]. Thus, MEP detection is limited to a single, localized region of the muscle, being sensitive to electrode position and neighbor muscle activation [6, 28]. In this case, if changes in coil orientation would also activate neighbor muscles with greater intensities [6, 46], then crosstalk could be biasing the effect of coil orientation on the target MEP amplitude.

A bi-dimensional grid of small electrodes with short inter-electrode distances, i.e. high-density electromyography [27], may be used to overcome the limited spatial information provided by conventional electrodes and cover the entire muscle extent [26]. For isotropic mediums, the detection volume of bipolar electrodes has been shown to approach well a semisphere with the radius proportional to the inter-electrode distance and centered midway between the electrodes [23]. Thus, considering the depth and transverse size of an intrinsic hand muscle, e.g. abductor pollicis brevis (APB; 0.68 ± 0.28 mm^2 cross-sectional area) [15], a smaller pick-up volume may provide greater specificity to better describe the location and distribution of motor units' myoelectric activity contribution to the muscle contraction elicited by TMS pulses.

Thus, this study investigated whether the amplitude distribution of MEPs elicited in the APB muscle is affected by the coil orientation. High-density electromyography has proven relevant for imaging MEPs over the entire muscle extent in TMS studies of the forearm [46] and arm muscles [19]. However, no previous studies assessed how MEPs are distributed over the entire extent of intrinsinc hand muscles of major interest in TMS studies. Following evidence from previous studies, MEP amplitude was expected to change equally across all channels in the grid, peaking for coil orientations corresponding to 45° with respect to the sagittal line [2, 4]. Alternatively, increasing TMS pulse intensity was suggested to activate motor neurons supplying fibers in different muscle regions [46], and changing pulse direction might well elicit distinct neuron populations [7, 12]. In this case, peaks in MEP amplitude would be observed in different muscle regions for different coil orientations, and sampling myoelectric activity from a single muscle region might provide a biased MEP view.

Materials and methods

Subjects

Thirteen subjects (three women and 10 men; 23–48 years old), all asymptomatic for neurological or motor disorders, participated in this study. The exclusion criteria for TMS were applied according to Rossi et al. [38]. All subjects gave written, informed consent prior to the beginning of the experiment. The experimental procedure was consistent with the Declaration of Helsinki and was approved by the institutional Ethics Committee (CEP-FFCLRP/USP 09697912.6.0000.5407).

MEP recordings

Surface electromyograms (EMGs) were recorded with a bi-dimensional array of 61 silver electrodes (13×5 pins; 1 mm diameter; 2.4 mm inter-electrode distance). Signals were pre-amplified with a gain of 500 or 1000, whichever provided the highest signal-to-noise ratio without saturation, by a multi-channel amplifier (10–500 Hz bandwidth, EMG-USB2 amplifier, OT Bioelettronica, Turin, Italy). The sampling frequency per channel, resolution and dynamic range for the A/D converter were 2048 Hz, 12 bits and ±2.5 V, respectively.

The electrode array was positioned with its center located over the APB muscle belly, following the recommendations of the project Surface Electromyography for Non-Invasive Assessment of Muscles (SENIAM) [42]. The central column of the grid was aligned along the axis defined from the muscle origin, at the scaphoid tubercle, to the muscle insertion, at the proximal phalange base of the thumb (dotted line at Figure 1A). The reference electrode was positioned over the wrist ipsilateral to the array. The skin surface was cleaned with alcohol and humidified with water to reduce the electrode-skin impedance.

Signals were processed using the software MEPHunter [43], developed in our lab and written in MATLAB version 8.1 R2013a (Math-Works, Natick, MA, USA). All EMGs were digitally filtered with a second-order bandpass Butterworth filter (10–500 Hz cutoff). MEPs were extracted from the EMGs detected by each electrode within 45-ms epochs, starting 15 ms after stimulation onset. All signals were visually inspected and EMGs where MEPs were not clearly identified were interpolated with its eight adjacent neighbors [45, 46]. An average of four to five channels in each map were interpolated.

Experimental design

The subjects wore a swim cloth cap and were seated comfortably in a reclining chair, with the neck, arms and hands fully relaxed. They

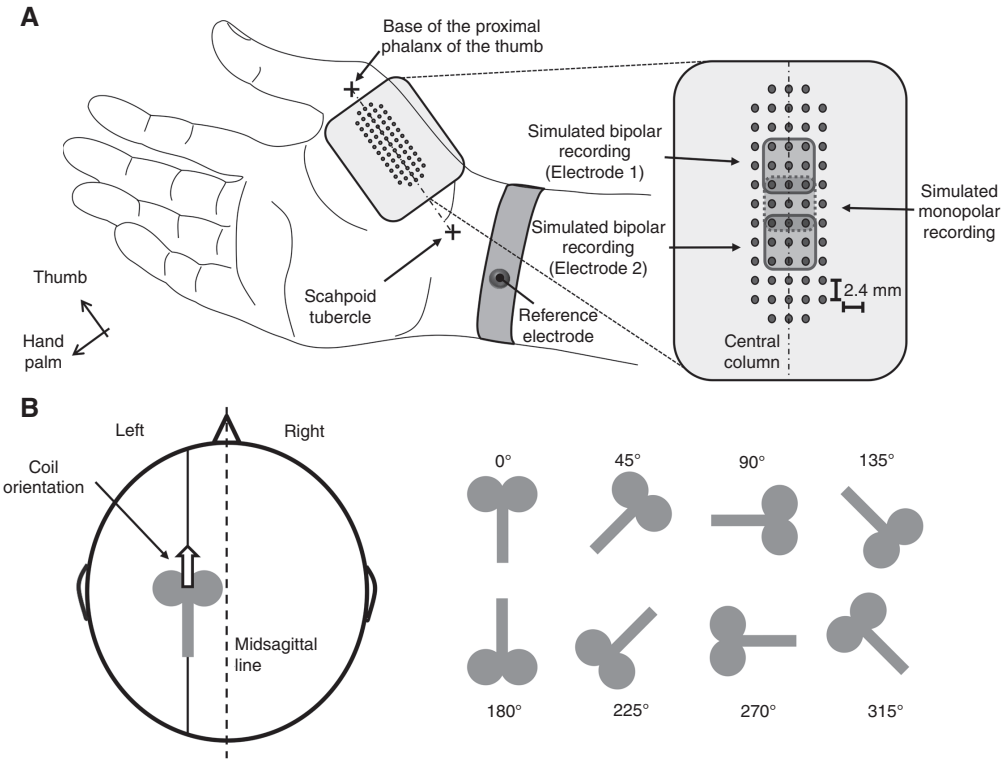

Figure 1: Electrodes and coil positioning.
(A) Schematic representation of the electrode array positioned over the APB muscle. The central column was aligned to the proximal phalanx of the thumb and the scaphoid tubercle. Hashed areas with solid contour line are the simulated electrodes of bipolar recording configuration [25 mm^2 contact area and 9.6-mm inter-electrode distance (IED)] and the hashed square area with dotted contour line is the electrode for simulated monopolar recording (25 mm^2 contact area). (B) Schematic representation of the eight TMS coil orientations with respect to the sagittal plane. The arrow points to the direction of the current flow through the coil, i.e. the posterior-anterior direction.

were advised to maintain the forearm in a neutral position throughout the experiment. TMS biphasic pulses were delivered to the APB motor hotspot with a figure-8 refrigerated coil (diameter of 75 mm at each winding; model MCF-B65) connected to the magnetic stimulator MagPro R30 (MagVenture, Faru, Denmark). For each participant, the APB hotspot was identified and marked on the cap as the cortical site beneath the coil center resulting in MEPs with maximum amplitude for a single TMS pulse [41, 53]. Then, the minimum stimulation intensity eliciting at least five out of 10 MEPs with amplitudes higher than 50 μV was identified as the motor threshold [5, 17]. Hotspots and motor thresholds were identified for both brain hemispheres, with coil orientation at 90° and current flowing in the lateral-medial direction (Figure 1B). MEPs considered in this procedure were obtained from the single-differential EMGs, taken along the central column of the array, and at least one MEP had to satisfy the conditions stated for the hotspots and motor thresholds.

Eight coil orientations were tested with angles varying in steps of 45°, with 0° corresponding to current flowing in the posterior-anterior direction ([2, 4]; Figure 1B). Ten pulses at 120% of individuals' motor threshold were delivered for each coil orientation [2]. The number of pulses was selected to assess each orientation during approximately 1 min and, therefore, ensure that coil tilt and orientation were kept constant. MEPs were visually inspected throughout the experiment. Stimulations were first applied to the right hemisphere (MEPs collected from the left APB). After approximately 10 min of rest, stimulations started for the left hemisphere and MEPs collected from the right APB. To avoid habituation, sequences of coil orientations were pseudo-randomized.

Data processing

Single-differential and monopolar maps were used to assess the effect of coil orientation on MEP amplitude spatial distribution. The center of the region where the highest MEPs were detected, i.e. the centroid of segmented electrodes, was defined by the weighted average of MEP amplitudes. All electrodes in the grid were considered to segment the cluster from monopolar MEPs, while in the single-differential derivation only electrodes located distally from the APB innervation zone were considered. The innervation zone was unambiguously identified as the row of electrodes providing MEPs with markedly low amplitude, interposed between rows providing clear MEPs with opposing phase [28]. Centroid coordinates along columns (X) and rows (Y) in the grid were specifically defined as:

$$X = \frac{1}{A}\sum_{i=1}^{c} x_i \sum_{j=1}^{r} a_{ij} \quad (1)$$

$$Y = \frac{1}{A}\sum_{j=1}^{r} y_j \sum_{i=1}^{c} a_{ij} \quad (2)$$

$$A = \sum_{i=1}^{c}\sum_{j=1}^{r} a_{ij} \quad (3)$$

where A is the sum of all amplitude values in the map and a_{ij} is the amplitude of MEPs detected by the electrodes with coordinates x_i and y_i. The X coordinate was then calculated as the percentage of total grid length in the column axis (medial-lateral direction) and the Y coordinate calculated as the percentage of total grid length in the row axis (proximal-distal direction).

Three detection systems were considered to assess the effect of coil orientation on MEP peak-to-peak amplitude (Figure 1A): (i) conventional monopolar recording; (ii) conventional bipolar recording; and (iii) monopolar recording provided by the grid of electrodes. Positioning and size of the monopolar and bipolar recording montages were also defined following SENIAM recommendations. First, MEPs were extracted from the resulting average of monopolar EMGs detected by electrodes in the grid between the sixth and the eighth rows and the second and the fourth columns. Averaging potentials recorded with multiple grid electrodes approximated the signal detected by large surface electrodes well, as described by Van Dijk et al. [45]. The selected arrangement led to a detection volume and a resulting MEP similar to that of monopolar recordings typically considered in TMS studies [6], hereafter called simulated conventional monopolar recording. In this study, the simulated square electrode encompassed a 25 mm^2 area over the central portion of the grid (dashed square shown in Figure 1A). Second, MEPs were collected from the difference of monopolar EMGs detected by two simulated square electrodes (25 mm^2 area and 9.6-mm inter-electrode distance; solid squares shown in Figure 1A). This method provided a detection volume and a resulting MEP as close as possible to that of conventional bipolar electrodes in TMS studies [6], hereafter called simulated conventional bipolar recording. Finally, MEPs obtained from a group of electrodes in the grid showing the greatest EMGs were considered for analysis. Initially, an automated method for the segmentation of EMGs was applied to identify where in the grid (i.e. cluster of electrodes) were MEPs most clearly represented [49]. Briefly, this method applies a watershed-based algorithm to identify groups of neighbor electrodes detecting EMGs greater than 70% of the grid's maximum amplitude; Figure 2 shows an example of MEP segmentation. The mean MEP amplitude across segmented electrodes was then calculated for each of the eight coil orientations.

Data and statistical analyses

The mean MEP amplitude across coil orientations and hemispheres of stimulation was calculated for each subject and EMG detection method, then defined as baseline. Subsequently, for each subject and detection method a relative MEP amplitude was calculated as the peak-to-peak amplitude for a given orientation divided by the baseline. Relative MEP amplitudes were divided into three groups according to the considered method of EMGs detection and then eight groups according to corresponding coil orientation. MEPs detected from the left APB muscle of one subject and from the right APB muscle of a second subject were discarded from the analysis due to strong TMS pulse artifacts during the MEP response, visually identified after 15 ms of stimulus delivery.

Statistical analysis was performed in R 3.3.0 [35]. A one-way analysis of variance (ANOVA) was used to test if coil orientation affects the centroid coordinates of each amplitude map. In addition, a two-way ANOVA was used to assess the effect of coil orientation and EMGs' detection modality on relative MEP amplitude. Post-hoc Tukey's honest significant difference was applied for multiple comparisons of conditions showing statistical significance. The level of significance was set at 5% for all tests. Results are presented as means and standard deviations.

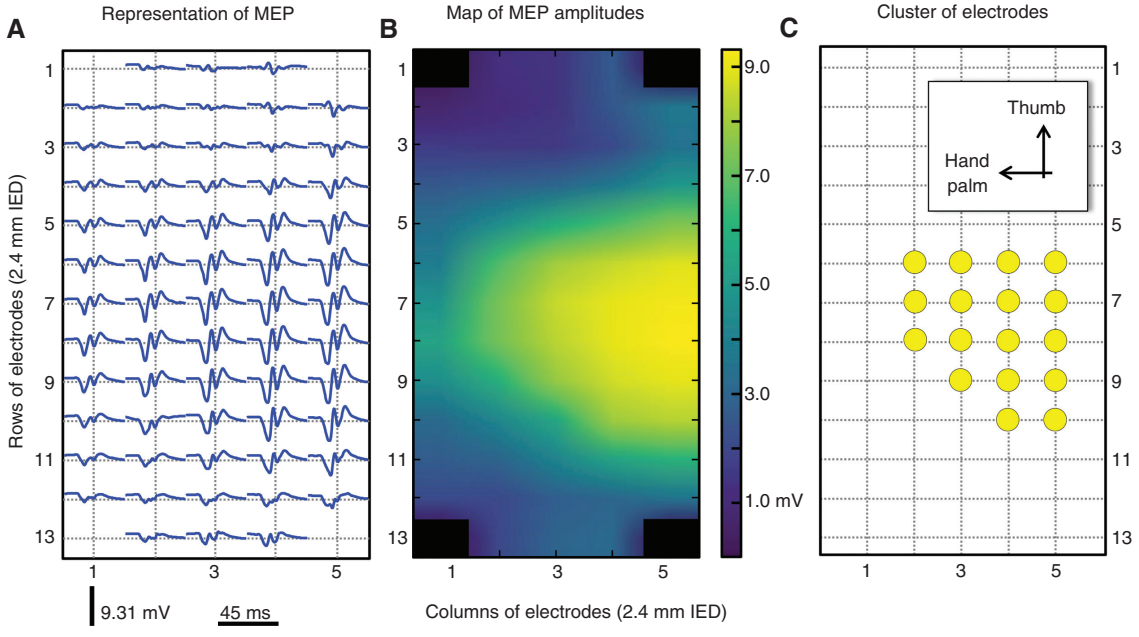

Figure 2: MEPs detected for stimulation at 45° over the left primary motor cortex (right hand) of one representative subject. (A) Spatial and temporal representation of monopolar MEPs detected for each electrode in the array. Higher MEPs are observed between the fifth and the tenth rows. (B) Scale image created with peak-to-peak amplitude of MEPs shown in (A). (C) Group of electrodes (yellow circles) from which higher MEPs in (A) were detected.

Results

Analysis of the amplitude distribution of monopolar maps showed that the centroid coordinates were not affected by the stimulus orientation on both medio-lateral [$F(7, 172) = 0.41$, $p = 0.892$] and proximo-distal axes [$F(7, 172) = 0.40$, $p = 0.903$]. The centroid of monopolar MEPs was located over the center of the grid in the

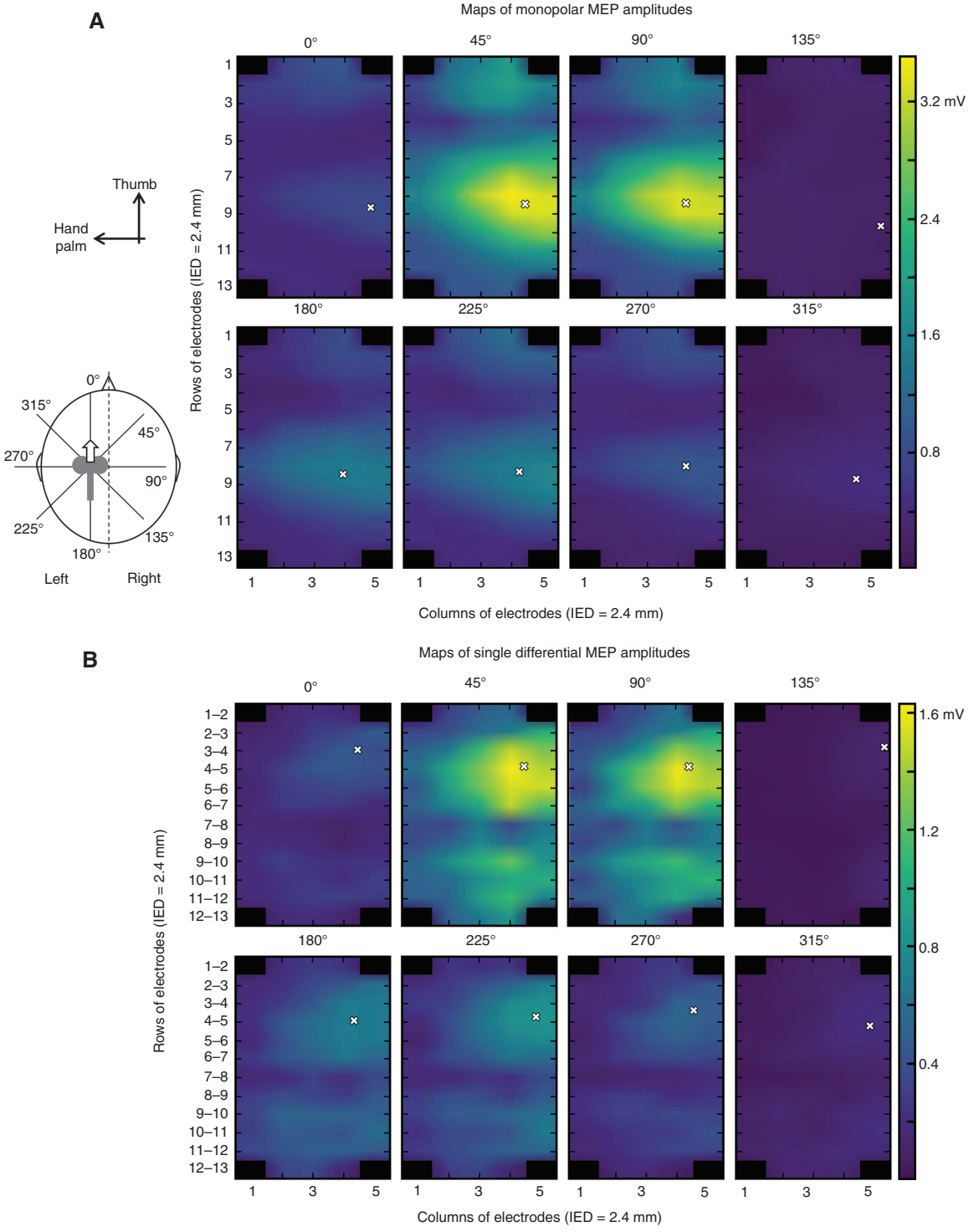

Figure 3: Scaled images created with peak-to-peak amplitude of monopolar (A) and single-differential (B) MEPs.
TMS was applied to the left hemisphere and EMGs recorded from the right APB of a representative subject. Centroids of amplitude distribution for each coil orientation are indicated with the white 'x'.

proximo-distal direction and slightly lateral for all coil orientations. Centroid X and Y coordinates averaged across subjects and coil orientations for monopolar maps were respectively located 62.7 ± 16.7% and 54.6 ± 18.2% from the top-left corner of the grid, as illustrated for a representative subject in Figure 3A. Likewise, centroid coordinates of differential MEPs did not change with coil orientation in both medio-lateral [$F(7, 151) = 0.35$, $p = 0.930$] and proximo-distal axes [$F(7, 151) = 0.33$, $p = 0.938$]. Mean centroid X and Y coordinates of differential maps across subjects and coil orientations were 64.8 ± 21.0% and 24.7 ± 10.22%, respectively, from the top-left corner of the grid (Figure 3B).

A two-way ANOVA revealed no statistically significant interaction between the effects of coil orientation and detection modality on MEP amplitude [$F(14, 552) = 0.217$, $p = 0.999$]. Yet, there was no main effect of detection modality on MEP amplitude [$F(2, 552) = 0.00$, $p = 1.00$]. However, a main effect of coil orientation on MEP amplitude was found for simulated mono- and bipolar recordings and segmented electrodes [$F(7, 552) = 62.07$, $p < 0.001$; Figure 4]. The greatest MEPs were obtained for TMS pulses applied at 45° when compared to all other coil orientations, regardless of the considered detection modality ($p < 0.05$). Monopolar and bipolar detection modalities also revealed the greatest MEP amplitude for 90° compared to other directions ($p < 0.05$). Cluster analysis showed that 0° also resulted in greater MEPs than 135°, 180°, 270° and 315° ($p < 0.05$). MEP amplitudes at 45° were at least two times higher than all other coil orientations, except at 90°. In addition, the smallest MEP amplitudes were detected for TMS stimuli delivered at 135° and 315°, approximately six times smaller than that evoked with the coil at 45°.

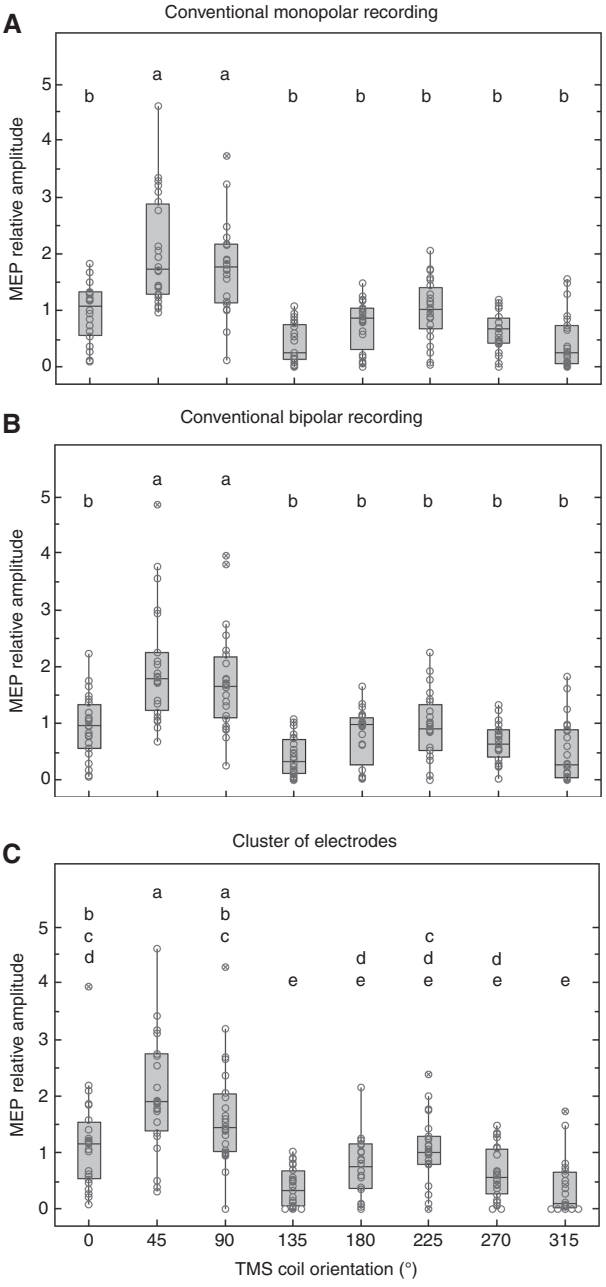

Figure 4: Boxplot of relative MEP amplitudes detected across all subjects and coil orientations.
Values refer to MEPs detected with monopolar (A), bipolar (B) and cluster of electrodes (C). The boxes' limits are the first and third quartiles, the center line is the median, the upper and lower lines are limits for outliers, the circles are MEP values and the marked circles are outlier MEP values. Lower letters (a, b, c, d, e) denote statistical difference ($p < 0.05$) after multiple comparisons with Tukey's test, where groups that do not share a letter are significantly different.

Discussion

In this study, we assessed whether TMS stimulus orientation affects the amplitude distribution of MEPs elicited for the APB, an intrinsic hand muscle. In addition, we investigated whether traditional electrode montages provide MEPs representative of global muscle activation for all coil orientations. For this purpose, MEPs were detected with a grid of electrodes covering the whole muscle extent. Extending findings from previous accounts, we observed that MEP amplitude distribution did not depend on the stimulus orientation and was centered at the same location for all coil orientations. Moreover, MEPs with equally higher amplitudes were detected with grids, bipolar and monopolar electrodes when current pulses were directed at 45° and 90°, but only the grid of electrodes revealed statistically significant coil orientations providing the smallest MEPs' amplitudes. These results suggest that traditional electrode montages may provide representative MEPs for the APB muscle and evidence that high-density

electromyography may contribute to better understanding supra-threshold TMS responses of the primary motor cortex.

Effect of coil orientation on MEP amplitude distribution

The centroid coordinates were used to extract information on the spatial distribution of myoelectric activity for different coil orientations. Centroid coordinates have different physiological interpretations though, depending on the relative position between electrodes in the grid and muscle fibers. When surface electrodes are positioned at skin regions covering the superficial extremities of muscle fibers pinnate in the depth direction, centroid coordinates change according to the location of active fibers beneath electrodes [29, 51]. The association between the location of active fibers within muscles pinnate in the depth direction and the amplitude distribution of surface EMGs holds both for single-differential and monopolar detections [29]. When EMGs are detected with electrodes positioned in a plane parallel to that of the muscle fibers, centroids have different meanings however, depending on the direction considered (i.e. parallel or transverse to muscle fibers) and on the detection modality. In a monopolar derivation, the location of centroids in the direction parallel to the muscle fibers coincides with the innervation zone location (Figure 2A); the amplitude of monopolar EMGs is greatest in correspondence to the innervation zone [18, 25]. In a differential derivation, the amplitude of EMGs is greatest for electrodes positioned between the innervation zone and the tendon regions [18]. This likely explains the differences in centroid coordinates along the thumb direction reported in Figure 3 for monopolar and differential detections. However, in a direction transverse to the muscle fibers, the centroid position is presumably associated with the distribution of active fibers along the transverse direction of the muscle's physiological cross-sectional area, regardless of whether EMGs are detected in monopolar or differential montages [13, 37]. Centroid shifts in the direction transverse to the thumb direction (Figure 1) would then be expected to reflect changes in the populations of motor units elicited for different TMS directions.

Changes in centroid position in the direction transverse to APB muscle fibers were not observed in both differential and monopolar MEPs (Figures 3 and 4). We assessed the MEP amplitude distribution for both detection derivations because both are typically considered in TMS studies [6]. The monopolar derivation has a larger pick-up volume [25] and, thus, monopolar EMGs are more sensitive to the activation of neighbor muscles (i.e. to crosstalk) than differential EMGs [9, 46] or other electrode arrangements [48]. In addition, the APB, the *flexor pollicis brevis* and the *opponens pollicis* muscles are partially overlapped in the thenar eminence and play an important role for the movement of the thumb. Therefore, changes in centroid position may be influenced by variations in active fibers within APB as well as in neighbor muscles. However, the short inter-electrode distance (2.4 mm) considered in the present study ensured a likely marginal contribution of action potentials elicited from fibers located at a radial distance greater than 2.4 mm from electrodes to the compound single-differential MEPs [23]. Variations in the transverse location of APB fibers elicited by changes in the coil orientation would then be expected to manifest in the transverse distribution of single-differential MEPs. The lack of a significant, transverse shift suggests however, that changes in MEP amplitude resulting from changes in coil orientation are not associated with the activation of populations of fibers in distinct APB muscle portions [31, 47] and may not depend on the activation patterns of the individual neighbor muscles.

Two key considerations should be made in the light of our results and interpretation. First, with the current approach we were not able to assess changes in the distribution of elicited muscle fibers in the depth direction. Changes in the coil orientation could have resulted in activation of distinct groups of motor neurons supplying predominantly deep or superficial APB muscle fibers [31, 47]. Differently from the medio-lateral centroid shifts, the association between changes in the centroid of MEP amplitude distribution and the location of active muscle fibers in the depth direction is not predictable for skin parallel-fibered muscles [37]. It is then possible to argue that changes in coil orientation have led to a differential recruitment of motor units supplying APB muscle fibers along the deep superficial region, not appreciated in the present study. Second, our current results may not be generalized to other muscles. Regional variations in activation have been observed both in intramuscular and surface recordings, for different conditions, e.g. TMS evoked responses [46], isometric and dynamic contractions, and for different muscles, with small and large physiological cross-sectional areas [10, 24, 50]. Even though the possibility of eliciting distinct APB muscle portions with TMS remains an open issue, our results revealed that MEP amplitude is highly sensitive to changes in coil orientation.

One limitation of our study is the non-navigated coil positioning. Even though neuronavigation has been shown to improve MEP reliability [16], the use of relatively

high stimulation intensity (i.e. 120% of the subject's motor threshold) and relatively coarse steps of 45° in coil orientation may overcome small fluctuations in coil positioning. However, we might not rule out the possibility that with fine navigated coil positioning and lower stimulation intensity it may be possible to improve muscle selectivity and thus investigate whether MEP amplitude spatial distribution varies with coil orientation with greater accuracy. Therefore, future studies might provide additional insights using navigated systems.

Optimal coil orientation to evoke representative MEPs in the APB muscle

The amplitude of MEPs elicited from the APB muscle depended markedly on the coil orientation. Even though different studies suggest an optimal, average coil orientation for which high, representative MEPs might be obtained from the APB muscle, there is conflicting evidence on the range of orientation values. Some accounts, for example, reported MEPs with the highest amplitudes when TMS pulses were delivered with the coil oriented 45° away from sagittal plane [4, 30, 33]. Others, however, suggest a range of orientation values between the antero-medial and latero-medial axes of the head for which MEPs with high amplitude might be obtained [1, 2, 36]. Our current results are more likely in agreement with these recent observations; we elicited MEPs with statistically high amplitudes for the 45° and 90° coil orientations (Figure 4).

The 45° range for optimal coil orientation, which provided the greatest MEPs, probably may result from the dual contribution of a high-induced electric field and neurons aligned in the direction of the stimulation fields. In the case of TMS for thenar muscles, tuning the coil to the antero-medial orientation apparently lead to an increase in the intensity of the induced electric field over the cortical tissue. However, high-induced electric fields may cause a loss of regional and physiological specificity of the TMS stimulus due to depolarization of a greater number of neural populations. This conjecture is supported by recent computational modeling [22, 32, 44] and experimental observations [12, 20, 21]. Yet, orienting the coil to 135° or 315° elicits the smallest MEP amplitudes, as indicated by the grid of electrodes' cluster analysis. This supports the idea, pointed out by previous studies [2, 44], that an induced electric field aligned perpendicular to neurons may be a non-effective arrangement for action potential discharges. Moreover, if the coil orientation would also affect the spatial distribution of MEPs over the APB muscle, it could be assessed by at least two orthogonal coil orientations, i.e. parallel (e.g. 45°) or perpendicular (e.g. 135°) to neuronal elements. Therefore, it is unlikely that changes in the spatial distribution of MEP amplitudes different from those observed in our study could be seen if a greater number of coil orientations were evaluated. Regardless of the potential factors accounting for a preferential coil orientation, TMS pulses oriented between 45° and 90° from the sagittal plane may consistently elicit the strongest MEPs while pulses oriented at a non-optimal coil orientation, i.e. 135° and 315°, may elicit the weakest muscle responses.

Do traditional electrode montages provide representative MEP amplitude?

Three detection modalities were considered to verify whether MEPs detected from the APB muscle depend on the electrode montage (Figure 1). The advantage of using grids of electrodes lies in the possibility of accounting for spatial variations in activity occurring within the muscle volume. More specifically, with grids of electrodes, we were able to track MEPs with highest peak-to-peak amplitudes regardless of where they were detected in the grid (Figures 2 and 3). Marked changes in the location of the greatest MEPs resulting from changes in coil orientation would therefore be expected to more substantially affect the conventional montages than the grid of electrodes, mainly in large and more compartimentalized muscles.

All detection modalities identified the same coil orientations to evoke maximum MEP amplitudes, i.e. 45° and 90° (Figure 4), but only the grid of electrodes statistically identified coil orientations that elicited the smallest muscle response, i.e. 135° and 315°. The difference between relative MEP amplitudes measured at optimal coil orientations compared to the others was much higher than the difference between amplitudes at non-optimal orientations compared to the others. Once cluster analysis only takes into account electrodes in the grid detecting the greatest amplitudes, it may be more sensitive to slight variations in MEP amplitude. In this sense, non-optimal coil orientations can consistently be isolated. However, simulated conventional monopolar and bipolar montages and grid of electrodes evidenced optimal coil orientations. One possible reason is the relatively large detection volume of our simulated, conventional electrodes compared to the size of the thenar muscles. Conventional montages are mostly sensitive to underlying muscle activity within the size of the active electrode, for monopolar recordings [25], and the inter-electrode distance, for bipolar recordings [23, 25]. As shown in Figure 1, both simulated electrodes covered most

of the APB extent, providing a relatively large detection volume. In addition, the detection volume of both monopolar and bipolar montages included the central portion of the grid, i.e. the muscle belly, where MEPs with the greatest amplitudes were located for all coil orientations, as evidenced by our centroid analysis. In summary, conventional electrodes may detect representative MEPs from thenar muscles at optimal coil orientations, while minor variations in amplitude at non-optimal orientations may only be detected with the grid of electrodes.

Conclusions

The effect of coil orientation on MEP amplitude distribution elicited from the APB muscle was assessed using a grid of electrodes. Distribution of MEPs is unlikely to be affected by coil orientation, with the greatest amplitudes being detected consistently by the same electrodes in the grid. Moreover, MEPs with the highest amplitudes might be elicited when the TMS coil is oriented 45°–90° away from the sagittal plan and the smallest amplitudes might be obtained at 135° and 315°. Representative MEPs may be equally detected with conventional mono- and bipolar electrodes at optimal coil orientation. Conversely, only the grid of electrodes seems to be sensitive to non-optimal orientations. Collectively, current results suggest that the coil orientation plays an important role in TMS applications and may be better assessed using high-density electromyography, in particular for large and more compartmentalized muscles.

Acknowledgments: The authors thank Breno R. G. Oliveira for statistical revision.

Funding: VHS was a recipient of a scholarship provided by Fundação de Amparo à Pesquisa do Estado de São Paulo (FAPESP; 2012/11937-0). This research has been conducted as part of the activities of FAPESP research, dissemination, and innovation center for Neuromathematics (grant 2013/07699-0). This work was also supported by Coordenação de Aperfeiçoamento de Pessoal de Nível Superior (CAPES).

Conflict of interest statement: Authors state no conflict of interest.

References

[1] Balslev D, Braet W, McAllister C, Miall RC. Inter-individual variability in optimal current direction for transcranial magnetic stimulation of the motor cortex. J Neurosci Methods 2007; 162: 309–313.

[2] Bashir S, Perez JM, Horvath JC, Pascual-Leone A. Differentiation of motor cortical representation of hand muscles by navigated mapping of optimal TMS current directions in healthy subjects. J Clin Neurophysiol 2013; 30: 390–395.

[3] Bembenek JP, Kurczych K, Karli Nski M, Czlonkowska A. The prognostic value of motor-evoked potentials in motor recovery and functional outcome after stroke – a systematic review of the literature. Funct Neurol 2012; 27: 79–84.

[4] Brasil-Neto JP, Cohen LG, Panizza M, Nilsson J, Roth BJ, Hallett M. Optimal focal transcranial magnetic activation of the human motor cortex: effects of coil orientation, shape of the induced current pulse, and stimulus intensity. J Clin Neurophysiol 1992; 9: 132–136.

[5] Conforto AB, Z'Graggen WJ, Kohl AS, Rösler KM, Kaelin-Lang A. Impact of coil position and electrophysiological monitoring on determination of motor thresholds to transcranial magnetic stimulation. Clin Neurophysiol 2004; 115: 812–819.

[6] Corneal SF, Butler AJ, Wolf SL. Intra- and intersubject reliability of abductor pollicis brevis muscle motor map characteristics with transcranial magnetic stimulation. Arch Phys Med Rehabil 2005; 86: 1670–1675.

[7] D'Ostilio K, Goetz SM, Hannah R, et al. Effect of coil orientation on strength-duration time constant and I-wave activation with controllable pulse parameter transcranial magnetic stimulation. Clin Neurophysiol 2016; 127: 675–683.

[8] Day BL, Dressler D, Maertens de Noordhout A, et al. Electric and magnetic stimulation of human motor cortex: surface EMG and single motor unit responses. J Physiol 1989; 412: 449–473.

[9] De Luca CJ, Kuznetsov M, Gilmore LD, Roy SH. Inter-electrode spacing of surface EMG sensors: reduction of crosstalk contamination during voluntary contractions. J Biomech 2012; 45: 555–561.

[10] Desmedt HE, Gidaux E. Spinal motoneuron recruitment in man: rank deordering with direction but not with speed of voluntary movement. Science 1981; 214: 933–936.

[11] Di Lazzaro V, Oliviero A, Saturno E, et al. The effect on corticospinal volleys of reversing the direction of current induced in the motor cortex by transcranial magnetic stimulation. Exp Brain Res 2001; 138: 268–273.

[12] Di Lazzaro V, Oliviero A, Pilato F, et al. The physiological basis of transcranial motor cortex stimulation in conscious humans. Clin Neurophysiol 2004; 115: 255–266.

[13] Gallina A, Vieira T. Territory and fiber orientation of vastus medialis motor units: a Surface electromyography investigation. Muscle Nerve 2015; 52: 1057–1065.

[14] Hallett M. Transcranial magnetic stimulation and the human brain. Nature 2000; 406: 147–150.

[15] Jacobson MD, Raab R, Fazeli BM, Abrams RA, Botte MJ, Lieber RL. Architectural design of the human intrinsic hand muscles. J Hand Surg Am 1992; 17: 804–809.

[16] Julkunen P, Säisänen L, Danner N, et al. Comparison of navigated and non-navigated transcranial magnetic stimulation for motor cortex mapping, motor threshold and motor evoked potentials. Neuroimage 2009; 44: 790–795.

[17] Kammer T, Beck S, Thielscher A, Laubis-Herrmann U, Topka H. Motor thresholds in humans: a transcranial magnetic stimulation study comparing different pulse waveforms, current

directions and stimulator types. Clin Neurophysiol 2001; 112: 250–258.
[18] Kleine BU, Schumann N-P, Stegeman DF, Scholle HC. Surface EMG mapping of the human trapezius muscle: the topography of monopolar and bipolar surface EMG amplitude and spectrum parameters at varied forces and in fatigue. Clin Neurophysiol 2000; 111: 686–693.
[19] Kleine B, Praamstra P, Zwarts M, Stegeman D. Impaired motor cortical inhibition in Parkinson's disease: motor unit responses to transcranial magnetic stimulation. Exp Brain Res 2001; 138: 477–483.
[20] Knecht S, Sommer J, Deppe M, Steinsträter O. Scalp position and efficacy of transcranial magnetic stimulation. Clin Neurophysiol 2005; 116: 1988–1993.
[21] Komssi S, Kähkönen S, Ilmoniemi RJ. The effect of stimulus intensity on brain responses evoked by transcranial magnetic stimulation. Hum Brain Mapp 2004; 21: 154–164.
[22] Laakso I, Hirata A, Ugawa Y. Effects of coil orientation on the electric field induced by TMS over the hand motor area. Phys Med Biol 2014; 59: 203–218.
[23] Lynn PA, Bettles ND, Hughes AD, Johnson SW. Influences of electrode geometry on bipolar recordings of the surface electromyogram. Med Biol Eng Comput 1978; 16: 651–660.
[24] McLean L, Goudy N. Neuromuscular response to sustained low-level muscle activation: within- and between-synergist substitution in the triceps surae muscles. Eur J Appl Physiol 2004; 91: 204–216.
[25] Merletti R, Lo Conte L, Avignone E, Guglielminotti P. Modeling of surface myoelectric signals. I. Model implementation. IEEE Trans Biomed Eng 1999; 46: 810–820.
[26] Merletti R, Holobar A, Farina D. Analysis of motor units with high-density surface electromyography. J Electromyogr Kinesiol 2008; 18 :879–890.
[27] Merletti R, Aventaggiato M, Botter A, Holobar A, Marateb H, Vieira TMM. Advances in surface EMG: recent progress in detection and processing techniques. Crit Rev Biomed Eng 2010; 38: 305–345.
[28] Mesin L, Merletti R, Rainoldi A. Surface EMG: the issue of electrode location. J Electromyogr Kinesiol 2009; 19: 719–726.
[29] Mesin L, Merletti R, Vieira TMM. Insights gained into the interpretation of surface electromyograms from the gastrocnemius muscles: a simulation study. J Biomech 2011; 44: 1096–1103.
[30] Mills KR, Boniface SJ, Schubert M. Magnetic brain stimulation with a double coil: the importance of coil orientation. Electroencephalogr Clin Neurophysiol 1992; 85: 17–21.
[31] Napier JR. The attachments and function of the abductor pollicis brevis. J Anat 1952; 86: 335–341.
[32] Opitz A, Legon W, Rowlands A, Bickel WK, Paulus W, Tyler WJ. Physiological observations validate finite element models for estimating subject-specific electric field distributions induced by transcranial magnetic stimulation of the human motor cortex. Neuroimage 2013; 81: 253–264.
[33] Pascual-Leone A, Cohen LG, Brasil-Neto JP, Hallett M. Non-invasive differentiation of motor cortical representation of hand muscles by mapping of optimal current directions. Electroencephalogr Clin Neurophysiol 1994; 93: 42–48.
[34] Pell GS, Roth Y, Zangen A. Modulation of cortical excitability induced by repetitive transcranial magnetic stimulation: influence of timing and geometrical parameters and underlying mechanisms. Prog Neurobiol 2011; 93: 59–98.
[35] R Core Team. R: a language and environment for statistical computing 2016.
[36] Richter L, Neumann G, Oung S, Schweikard A, Trillenberg P. Optimal coil orientation for transcranial magnetic stimulation. PLoS One 2013; 8: 1–10.
[37] Roeleveld K, Stegeman DF, Vingerhoets HM, Van Oosterom A. The motor unit potential distribution over the skin surface and its use in estimating the motor unit location. Acta Physiol Scand 1997; 161: 465–472.
[38] Rossi S, Hallett M, Rossini PM, Pascual-Leone A, Safety of TMS Consensus Group. Safety, ethical considerations, and application guidelines for the use of transcranial magnetic stimulation in clinical practice and research. Clin Neurophysiol 2009; 120: 2008–2039.
[39] Rossini PM, Rossi S. Clinical applications of motor evoked potentials. Electroencephalogr Clin Neurophysiol 1998; 106: 180–194.
[40] Rossini PM, Burke D, Chen R, et al. Non-invasive electrical and magnetic stimulation of the brain, spinal cord, roots and peripheral nerves: basic principles and procedures for routine clinical and research application. An updated report from an I.F.C.N. Committee. Clin Neurophysiol 2015; 126: 1071–1107.
[41] Säisänen L, Pirinen E, Teitti S, et al. Factors influencing cortical silent period: optimized stimulus location, intensity and muscle contraction. J Neurosci Methods 2008; 169: 231–238.
[42] SENIAM project (Surface Electromyography for the Non-Invasive Assessment of Muscles) n.d. http://www.seniam.org/ (accessed September 12, 2015).
[43] Souza VHO, Peres ASC, Baffa O. MEPHunter 2015. https://github.com/biomaglab/mephunter (accessed September 12, 2015).
[44] Thielscher A, Opitz A, Windhoff M. Impact of the gyral geometry on the electric field induced by transcranial magnetic stimulation. Neuroimage 2011; 54: 234–243.
[45] Van Dijk JP, Lowery MM, Lapatki BG, Stegeman DF. Evidence of potential averaging over the finite surface of a bioelectric surface electrode. Ann Biomed Eng 2009; 37: 1141–1151.
[46] Van Elswijk G, Kleine BU, Overeem S, Eshuis B, Hekkert KD, Stegeman DF. Muscle imaging: mapping responses to transcranial magnetic stimulation with high-density surface electromyography. Cortex 2008; 44: 609–616.
[47] Van Sint Jan S, Rooze M. The thenar muscles. Surg Radiol Anat 1992; 14: 325–329.
[48] van Vugt JP, van Dijk JG. A convenient method to reduce crosstalk in surface EMG. Cobb Award-winning article, 2001. Clin Neurophysiol 2001; 112: 583–592.
[49] Vieira TMM, Merletti R, Mesin L. Automatic segmentation of surface EMG images: improving the estimation of neuromuscular activity. J Biomech 2010; 43: 2149–2158.
[50] Vieira TMM, Loram ID, Muceli S, Merletti R, Farina D. Postural activation of the human medial gastrocnemius muscle: are the muscle units spatially localised? J Physiol 2011; 589: 431–443.
[51] Vieira TM, Botter A, Minetto MA, Hodson-Tole EF. Spatial variation of compound muscle action potentials across human gastrocnemius medialis. J Neurophysiol 2015; 114: 1617–1627.
[52] Wassermann EM, Zimmermann T. Transcranial magnetic brain stimulation: therapeutic promises and scientific gaps. Pharmacol Ther 2012; 133: 98–107.

[53] Wassermann EM, McShane LM, Hallett M, Cohen LG. Noninvasive mapping of muscle representations in human motor cortex. Electroencephalogr Clin Neurophysiol 1992; 85: 1–8.
[54] Werhahn KJ, Fong JK, Meyer BU, et al. The effect of magnetic coil orientation on the latency of surface EMG and single motor unit responses in the first dorsal interosseous muscle. Electroencephalogr Clin Neurophysiol 1994; 93: 138–146.
[55] Ziemann U. Transcranial magnetic stimulation: its current role in the evaluation of patients post-stroke. J Neurol Phys Ther 2000; 24: 82–93.